JOURNAL OF CATALYSIS 149, 117–126 (1994)

Relationships between Microstructure and Surface Acidity of Ti–Si Mixed Oxide Catalysts

Zhufang Liu, Jose Tabora, and Robert J. Davis[1]

Department of Chemical Engineering, University of Virginia, Charlottesville, Virginia 22903-2442

Received February 15, 1994; revised April 29, 1994

The surface acidities and reactivities of titania, silica, and a series of Ti–Si mixed oxides have been investigated with a variety of surface-sensitive techniques, including temperature-programmed desorption/reaction of ammonia and 2-propanol, IR spectroscopy of adsorbed ammonia, and catalytic reaction of 1-butene. Results from TPD, TPR, and IR spectroscopy indicated that total acidity and relative acid strength decreased as silica was incorporated into titania. However, the areal rate of 1-butene isomerization was almost four times greater over a titania-rich mixed oxide than over pure titania. Infrared spectroscopy of adsorbed ammonia revealed that all of the acid sites on pure titania were of the Lewis type, whereas about 80% of the sites on the mixed oxides were of the Brønsted type. Therefore, the enhancement of butene isomerization activity over titania-rich mixed oxides was attributed to the Brønsted acid sites that were not present on pure titania. The appearance of Brønsted acidity in titania-rich mixed oxides was due to the local charge imbalance associated with tetrahedrally coordinated silica chemically mixing with the octahedral titania matrix. In silica-rich mixed oxides, Ti substituted isomorphously for Si in the tetrahedral silica matrix, thus eliminating the local charge imbalance that caused Brønsted acidity. The molar ratio of $NH_{3(ads)}$/Ti for a silica-rich mixed oxide was approximately 0.3, which was nearly the same as the fraction of nontetrahedrally coordinated Ti in the sample.

INTRODUCTION

Titania–silica mixed oxides are important catalysts and catalyst supports. For example, silicas containing small quantities of titanium are used as catalysts for the selective epoxidation of alkenes by organic hydroperoxides (1, 2). At higher Ti concentrations, the mixed oxides exhibit substantial surface acidities; thus, they are active for acid-catalyzed reactions such as phenol amination (3), ethene hydration (3), butene isomerization (3, 4, 5), cumene dealkylation (6), 2-propanol dehydration (6), and 1,2-dichloroethane decomposition (7). Since the unique chemical and physical properties of titania–silica binary oxides depend on both the composition and the degree of homogeneity, synthesis techniques have been developed to prepare the mixed oxides in a uniform manner, including coprecipitation (3, 4, 6), flame hydrolysis (8), and sol–gel hydrolysis (9, 10). In fact, high-surface-area aerogels and xerogels can be synthesized by precisely controlling hydrolysis conditions and drying procedures (11). Although methods for preparing mixed oxides have greatly improved, relationships between mixed oxide structure and chemical reactivity remain elusive, mostly because chemically mixed Ti–Si oxides are noncrystalline and therefore difficult to study.

In an earlier paper, we described the microstructural characteristics of a series of microporous titania–silica mixed oxides prepared by liquid-phase hydrolysis of titanium isopropoxide and tetraethyl orthosilicate (12). Since X-ray diffraction indicated that the final calcined materials were amorphous, techniques including X-ray absorption, UV reflectance, laser Raman, and FT-IR absorption spectroscopies were used to derive information on the local environment of Ti atoms in the powders. We found that the microstructure of the Ti oxide component depends on the overall elemental composition of the mixed oxide since the addition of Si increases the concentration of TiO_4 relative to TiO_6 structural units. As expected, Ti isomorphously substitutes in the tetrahedral silica framework of silica-rich mixed oxides. Results from the various techniques indicated that the Ti–O bond contracted with silicon incorporation and that Ti–O–Si linkages formed in the mixed oxides. The relatively high Ti loadings in the samples precluded the observation of isolated TiO_4^{4-} tetrahedra formed by substitution of Ti into the silica network. However, a sample containing about 11 at.% titania consists of small Ti-rich domains, less than 1 nm in size, which contain several tetrahedrally coordinated Ti oxide structural units possibly linked to a single octahedrally coordinated Ti oxide unit.

In this work, we examined the surface characteristics of the same Ti–Si mixed oxides used for the microstructure study. Temperature-programmed desorption of ammonia,

[1] To whom correspondence should be addressed.

0021-9517/94 $6.00

temperature-programmed reaction of 2-propanol, catalytic isomerization of 1-butene, and FT-IR spectroscopy of adsorbed ammonia were used to evaluate the acidity and reactivity of the mixed oxide surfaces. Structure–property relationships describing the surface acidity of Ti–Si mixed oxides are based on the results from both surface- and bulk-phase characterization.

EXPERIMENTAL METHODS

Materials Synthesis

The samples in this work are the same as those described in a previous paper (12). As an example, the synthesis of a Ti–Si binary oxide with a 1 : 1 Ti : Si molar ratio is described below. All other samples were prepared in an analogous fashion. About 15 g of tetraethyl orthosilicate (Aldrich, 99%) and 20 g of titanium(IV) isopropoxide (Aldrich, 97%) were added to 100 ml of 2-propanol (Fisher, purified grade, dried over molecular sieves). Then, 11 ml of distilled, deionized water were injected over the course of 1 h into the well-agitated system at room temperature using a syringe pump (Sage Instruments, Model 355). The solvent was allowed to slowly evaporate from the system at room temperature. After about 5 h, a white powder was obtained which was further dried in air at 383 K for 10 h. Final calculation was performed in air at 673 K for 4 h. Mixed oxide samples are designated by the atomic ratio of Ti to Si, e.g., Ti : Si 1 : 1. Pure titania and pure silica were prepared in the same way as the mixed oxides, except that only a single alkoxide precursor was placed in the reactant solution. In some experiments, a commercial titania sample (Degussa P25) having a surface area of 50 $m^2 g^{-1}$ was also used. Surface areas of the calcined materials were calculated from dinitrogen adsorption isotherms using the BET formalism.

Temperature-Programmed Desorption of Ammonia

Temperature-programmed desorption (TPD) of preadsorbed ammonia from the catalysts was used to estimate the density of surface acid sites. An atmospheric pressure flow system with a quadrupole mass spectrometer was used for the experiment. First, a fresh 150-mg sample was heated at a rate of 4 K min^{-1} in flowing He (Roberts Oxygen, 99.999%) and then calcined in He for 4 h at 673 K. Following calcination, the sample was cooled to 373 K and exposed to an equimolar mixture of He and NH_3 (Robert Oxygen, 99.999%) flowing for 0.5 h. The system was then purged with He for 4 h at 373 K to remove weakly adsorbed ammonia. The temperature of the sample was increased linearly by 10 K min^{-1} to desorb ammonia from the catalyst surface into the He carrier stream (57 STP cm^3 min^{-1}) while the NH_3 concentration in the gas phase was monitored with the mass spectrometer. The amount of ammonia desorbed was quantified by comparing the area under the TPD curve to peak areas of ammonia calibration pulses injected after each experiment.

Temperature-Programmed Reaction of 2-Propanol

The temperature-programmed reaction (TPR) of 2-propanol was performed with the same atmosphere pressure flow system as that used for ammonia TPD. A 50-mg sample was first calcined at 673 K for 4 h in He. The catalyst was then cooled to room temperature, RT, and exposed for 30 min to a flowing mixture of He and 2-propanol (Fisher Scientific, HPLC grade) obtained from a saturator maintained at 273 K. The system was then purged with flowing He for 1 h at RT to remove weakly adsorbed 2-propanol. The TPR occurred during heating in flowing He (37 STP cm^3 min^{-1}) at a rate of 10 K min^{-1}. The desorption of unreacted 2-propanol (masses 45 and 43) and formation of propene (mass 41) were monitored with the mass spectrometer. Calibration pulses of 2-propanol and propene were injected during each experiment. The contributions of each species to the total signals for masses 45, 43, and 41 allowed for quantification of the amounts of each product evolved. No propanone was observed during any of the experiments.

Isomerization of 1-Butene

The isomerization of 1-butene was studied using a closed-loop recirculation system with a total volume of 1.2 liters. A 150-mg sample was cooled to room temperature following activation in flowing He at 673 K for 4 h, and the entire system was evacuated to 10^{-5} mbar. After isolating the reactor, 190 mbar of 1-butene (Aldrich, 99%) was added to the system. Three freeze–pump–thaw cycles removed any gaseous impurity in the 1-butene. After butene purification, He was added to bring the total pressure to atmospheric. The 1-butene/He mixture was circulated over the catalyst at 423 K and 10-μl samples were withdrawn by an in-line sampling valve to be analyzed by gas chromatography. The only products detected were *cis*-2-butene and *trans*-2-butene.

FT-IR Spectroscopy of Adsorbed Ammonia

The IR absorbance spectra were collected in the transmission mode using a BioRad FTS 60A FT-IR spectrometer equipped with an *in situ* heatable IR cell (Harrick HTC-100). Thin catalyst pellets were prepared without the use of binder. During a standard experiment, the sample was first calcined in flowing dinitrogen (Roberts Oxygen, 99.99%) at 673 K for 4 h in order to directly compare the results with those obtained from ammonia TPD, 2-propanol TPR, and catalytic reaction. After cooling the cell to 373 K, flowing ammonia (300 mbar) was passed

TABLE 1

Adsorption Capacities of Ti–Si Mixed Oxides for Ammonia and 2-Propanol

Sample	Ti : Si atomic ratio	Surface area ($m^2\ g^{-1}$)	NH_3 uptake (10^6 mol m^{-2})	2-Propanol uptake (10^6 mol m^{-2})	2-Propanol reacted (%)
TiO_2	—	100	3.2	6.3	59
Ti : Si, 6 : 1	5.72 : 1	310	2.4	3.8	72
Ti : Si, 4 : 1	3.16 : 1	410	2.3	3.8	58
Ti : Si, 1 : 1	1 : 1.08	450	2.1	3.9	36
Ti : Si, 1 : 4	1 : 4.79	470	1.8	3.8	22
Ti : Si, 1 : 8	1 : 8.20	410	1.4	3.2	16
SiO_2	—	390	Trace	Trace	Trace

over the sample for 30 min. The cell was subsequently purged with flowing N_2 for 4 h to remove weakly adsorbed ammonia and an IR spectrum was recorded. After purging for an additional 4 h, the sample was heated by 10 K, held at that temperature for 4 h in flowing dinitrogen, and cooled back to 373 K for acquisition of another spectrum. This same sequence was repeated at 10-K intervals up to 453 K. All spectra were collected at 373 K and averaged from 256 scans with a resolution of 4 cm^{-1}.

RESULTS

The elemental compositions of the mixed oxides were similar to the nominal compositions of the starting solutions, as shown in Table 1. After calcination at 673 K, the powders revealed exceptionally high surface areas, approaching 500 $m^2\ g^{-1}$ in some cases. The surface area of the most Ti-rich mixed oxide, Ti : Si 6 : 1, was three times greater than that of pure titania, which illustrates the stabilizing effect on surface area of a small quantity of Si.

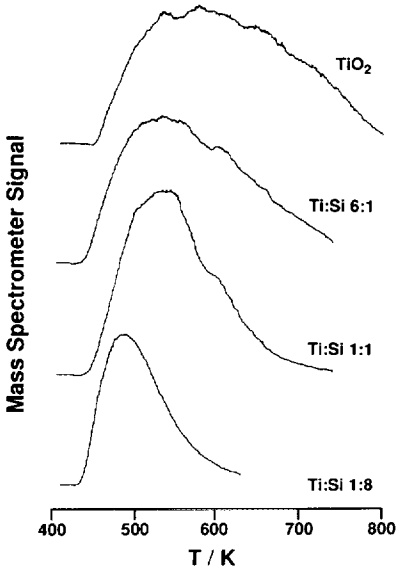

FIG. 1. Results from temperature-programmed desorption of ammonia from titania and Ti–Si mixed oxides.

Representative curves from the temperature-programmed desorption of ammonia are plotted in Fig. 1. The very broad desorption features associated with titania and the titania-rich mixed oxide indicate that stronger adsorbate–surface interactions occur on these materials than on the silica-rich mixed oxides. Evidently, the acid strength of a mixed oxide decreases with increasing silica content. In fact, no ammonia desorbed from a pure silica surface. However, care must be exercised when TPD results from microporous materials are interpreted since severe readsorption can occur during the experiment. Additional information on the bond strength of ammonia to the surface was provided by FT-IR spectroscopy, which is discussed later. The TPD curves also provided a measure of the total adsorption capacities of the samples for ammonia. The NH_3 uptake values in Table 1 indicate that titania adsorbed the greatest amount of ammonia and that the adsorption capacity decreased with increasing silica content.

We also probed the surfaces of the mixed oxides with the temperature-programmed reaction of 2-propanol to propene. Representative curves from the TPR of 2-propanol, illustrated in Fig. 2, show that unreacted 2-propanol desorbed at relatively low temperatures, whereas propene desorbed at about 450–500 K. In addition, the fraction of 2-propanol that reacted to form propene was greatly affected by the composition of the mixed oxide. Silica-rich mixed oxides converted the lowest amounts of alcohol. No 2-propanol or propene desorbed from a pure silica surface over the temperature range depicted in Fig. 2. Table 1 lists the total amounts of 2-propanol adsorbed (the sum of the moles of 2-propanol and propene desorbed) and the percentage conversion of 2-propanol to propene over the various samples. We also performed 2-propanol TPR on Degussa P25 and found that this commercial sample

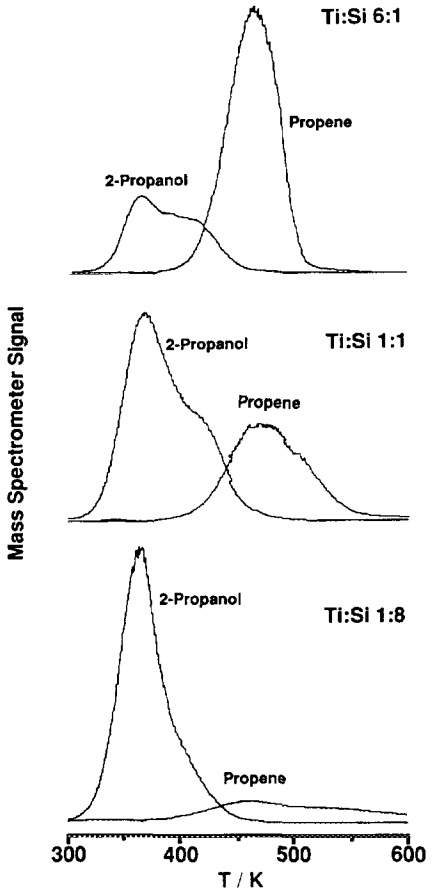

FIG. 2. Results from the temperature-programmed reaction of 2-propanol on Ti–Si mixed oxides.

adsorbed 4.5×10^{-6} mol m^{-2} of 2-propanol and converted 70% to propene.

The oxides also catalyzed the isomerization of 1-butene to form cis- and *trans*-2-butenes. The *cis/trans* ratios of the product butenes extrapolated to 0% conversion are given in Table 2. For each catalyst, the *cis/trans* ratio was near unity. The initial rate of isomerization is plotted

TABLE 2

Ratio of 2-Butene Products from 1-Butene Isomerization over Ti-Containing Oxides

Sample	*cis/trans* Ratio[a]
TiO_2	2.5
Ti : Si, 6 : 1	2.0
Ti : Si, 1 : 1	1.8
Ti : Si, 1 : 8	1.3

[a] Values were calculated from rates measured at 423 K and extrapolated to 0% conversion.

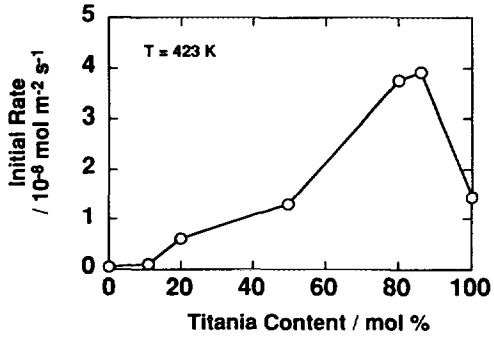

FIG. 3. Influence of catalyst composition on the specific rate of 1-butene isomerization.

as a function of oxide composition in Fig. 3. The most active sample was a Ti-rich mixed oxide whereas the least active sample was pure silica. Interestingly, the Ti : Si 6 : 1 catalyst was almost four times more active than pure titania.

The IR absorption spectra of the hydroxyl region of the freshly calcined samples are shown in Fig. 4. The pure silica sample and the silica-rich materials exhibited a single, high-wavenumber peak at 3740 cm^{-1} associated with isolated surface hydroxyl, or silanol, groups (13). The pure titania and Ti : Si 6 : 1 samples, however, revealed

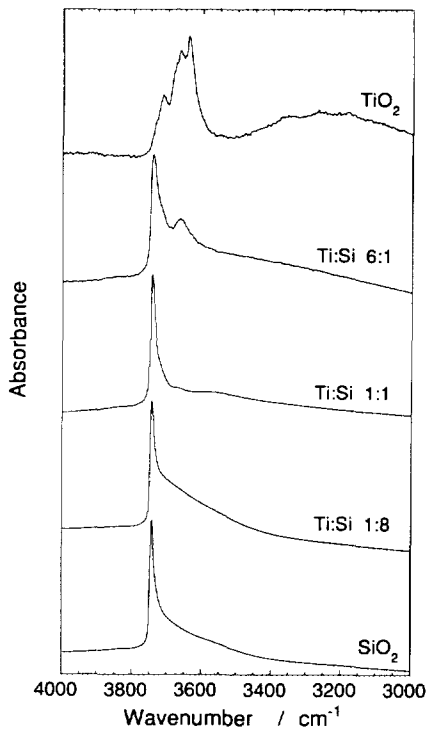

FIG. 4. Infrared absorption spectra of oxide samples. All of the samples were treated *in situ* at 673 K, except silica, which was treated at 573 K.

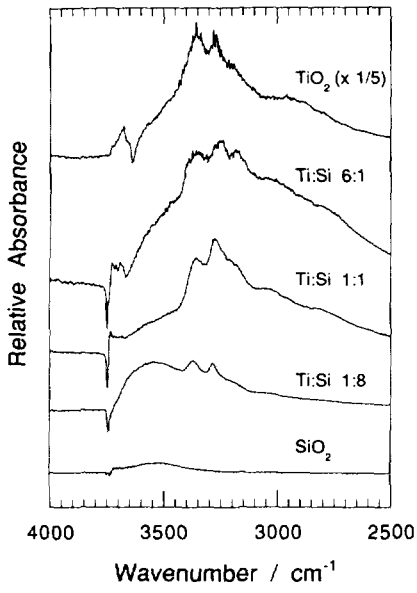

FIG. 5. Infrared spectra of ammonia adsorbed on the oxide samples represented in Fig. 4. The spectrum of each oxide sample has been subtracted.

additional peaks at lower wavenumbers (3716, 3666, and 3640 cm^{-1}). Previous researchers have already reported that several hydroxyl bands are present in the spectrum of titania. For example, Primet *et al.* observed multiple bands on anatase (3715, 3665 cm^{-1}) and on rutile (3685, 3655 cm^{-1}) (14). For both samples, the low-wavenumber band was assigned to hydrogen-bonded hydroxyl groups, whereas the high-wavenumber band was assigned to isolated hydroxyl groups (14). However, others have attributed the high-wavenumber band on titania to a silica impurity in the sample (13, 15).

The hydroxyl region is greatly perturbed by the adsorption of ammonia on the samples. In Fig. 5, the spectra of the fresh samples have been subtracted from the spectra of the samples after ammonia adsorption so that the negative peaks indicate the disappearance of isolated hydroxyl groups on the ammonia-cover surfaces. The peaks located from 3400 to 3000 cm^{-1} result from symmetric and asymmetric NH stretches of adsorbed ammonia (16). As shown in Fig. 5, the spectrum for ammonia on titania exhibits broad bands at 3356 and 3280 cm^{-1} with shoulders at 3400 and 3190 cm^{-1}. The spectrum for Ti : Si 6 : 1 has broad bands at 3348, 3248, and 3183 cm^{-1} whereas the spectrum for Ti : Si 1 : 1 has features at 3354, 3275, and 3200 cm^{-1}. The spectrum for the silica-rich sample, Ti : Si 1 : 8, reveals only two well-defined bands at 3374 and 3285 cm^{-1}. Primet *et al.* (17) and Dines *et al.* (18) observed four bands in the NH stretching region of the IR spectrum of ammonia adsorbed on titania. They assigned the four bands to the symmetric and asymmetric stretches of ammonia adsorbed on two different types of Lewis acid sites. Likewise, the multiple bands associated with titania and some of the mixed oxide samples in this work suggest that more than one type of Lewis acid site is present on the surfaces. Also, the two bands in Fig. 5 for Ti : Si 1 : 8 indicate that only a single type of Lewis acid interaction with ammonia is present on the silica-rich sample.

The wavenumber region of the spectrum from 1700 to 1300 cm^{-1} is more informative than the high-wavenumber region for evaluating the number densities of Lewis and Brønsted acid sites on the mixed oxide surfaces. Figure 6 shows the two well-resolved peaks associated with ammonia adsorbed on a surface cation, or Lewis acid site (1605 cm^{-1}), and the ammonium ion resulting from adsorption on a Brønsted site (1430 cm^{-1}). The spectra in Fig. 6 are normalized by the surface areas of the sample pellets so that the peak areas of each type of acid site on the different materials can be compared. However, the Brønsted peak areas cannot be directly compared to the Lewis peak areas without also considering the different extinction coefficients. The IR spectrum of ammonia on pure titania in Fig. 6 indicates that only Lewis acid sites are accessible for ammonia adsorption. Apparently, the hydroxyl groups on pure titania are not able to protonate ammonia under the conditions of this study. The intensity of the Lewis acid peak for titania was so large that the spectrum was reduced by a factor of 5 before being included in Fig. 6. The large difference in the areas of the peaks at 1605 cm^{-1} for titania and Ti : Si 6 : 1 indicates that a relatively small amount of silica suppressed a major

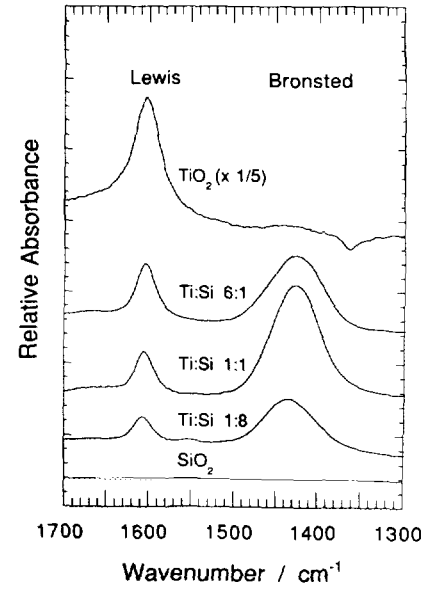

FIG. 6. Low-wavenumber IR spectra of ammonia adsorbed on oxides.

fraction of the Lewis acid sites normally associated with titania.

The relationship between integrated IR peak area and ammonia desorption temperature was used to evaluate the strength of the adsorbate–surface interaction. Figure 7a illustrates the decrease in the Lewis peak intensity as the desorption temperature increases. Almost no ammonia remained adsorbed on mixed oxide Lewis acid sites at 453 K, whereas about half of the ammonia remained on pure titania at the same temperature. Figure 7b shows the decrease in the Brønsted peak intensity with increasing temperature for the mixed oxides. Ammonia desorbed almost completely from the Brønsted sites at 453 K, which is similar to the desorption from Lewis sites. Therefore, results from both TPD and IR spectroscopy are consistent and show that ammonia is bound more strongly to the acid sites on pure titania than any of the mixed oxides. The relatively low temperatures used to remove ammonia during stepwise desorption in the IR cell indicate the influences of microporosity and thermal nonuniformities on the ammonia TPD curves in Fig. 1. Therefore, ammonia TPD was used only to measure the total acidity of the samples and to confirm the ranking of acid strengths determined from the IR study.

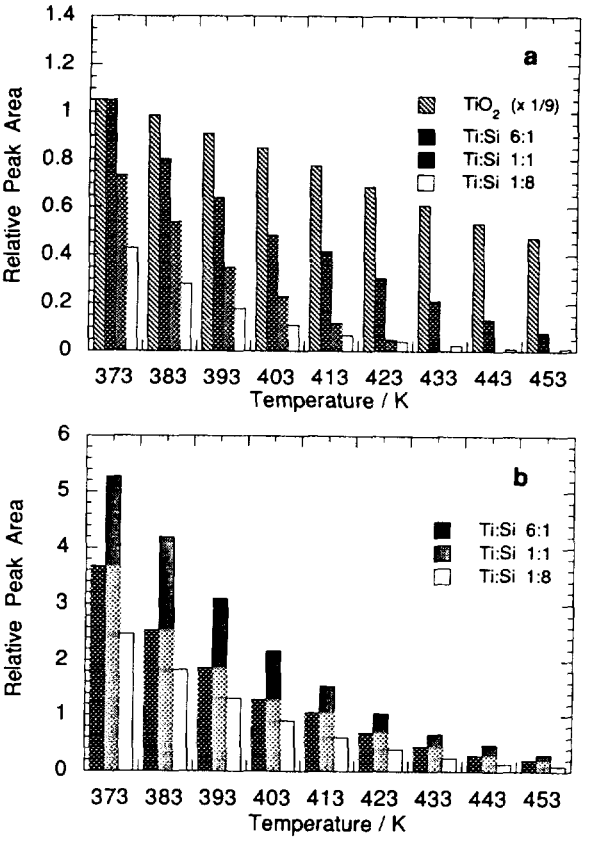

FIG. 7. Influence of desorption temperature on the integrated IR peak areas associated with ammonia adsorbed on (a) Lewis acid sites and (b) Brønsted acid sites.

DISCUSSION

Since a complete discussion on the microstructure of these Ti–Si mixed oxide samples can be found in Ref. (12), we will discuss only the surface characterization of the materials and the relationships between the microstructure and acidity.

Total acidities were estimated from ammonia TPD and the results are shown in Table 1. The highest density of acid sites was 3.2×10^{-6} mol m^{-2} for pure titania, which compares to 5.8×10^{-6} (19), 1.5×10^{-6} (20), and $2.9–3.6 \times 10^{-6}$ mol m^{-2} (21) determined by a variety of acid titration methods on titania. We observed a decrease in the number density of surface acid sites with increasing silica content as shown in Table 1. Nakabayashi (5) and Odenbrand *et al.* (19) also found lower surface acidities on the mixed oxides relative to titania. However, others have found the opposite result (4, 20, 22). Evidently, no clear consensus exists to describe the trend in number density of surface acid sites on Ti–Si mixed oxides.

In addition to number density, the strength of the acid site plays an important role in catalysis. The ammonia TPD curves could indicate that the strongest acid sites are present on pure titania, and that acidity progressively weakens as Si is incorporated. However, ammonia TPD cannot be used to unambiguously rank materials according to acid strength because basic solids like CaO can also adsorb ammonia quite strongly (23). Therefore, we performed a version of the TPD experiment in the IR spectrometer in order to observe directly the interaction of ammonia with surface acid sites. As depicted in Fig. 7, ammonia associated with both Brønsted and Lewis sites was adsorbed less strongly on the silica-rich materials. This experiment conclusively shows that the acid strengths of the mixed oxides decrease with increasing silica content, which is entirely consistent with the lack of significant surface reactivity of the silica-rich mixed oxides for 1-butene isomerization and 2-propanol dehydration. This conclusion is also supported by the high-wavenumber region of the IR spectra of adsorbed ammonia (Fig. 5). The broad feature associated with weak hydrogen bonding of the surface OH groups with ammonia occurs at higher wavenumbers on the Ti : Si 1 : 8 than on the titania-rich samples, indicating that the Brønsted sites are weaker on the silica-rich sample (19). In contrast to our results, other researchers have observed strong acid sites on silica-rich samples (3, 4, 19, 20, 22). Again, no clear consensus exists regarding the distribution of acid strengths on mixed oxides prepared in different laboratories. Recently, strong acid sites ($H_0 = -5.6$) have been detected on pure titania that has a very small particle size

(24). Therefore, the preparation method of titania can greatly affect the resulting surface acidity. Since our titania sample has a fairly high surface area and is poorly crystallized, strong acid sites should be present.

In order to investigate the relative acidities and reactivities of the oxides without the inherent ambiguities associated with using ammonia, we performed the temperature-programmed dehydration of 2-propanol. This technique has been used previously to measure the titania surface areas of mixed oxides of titania and silica (25). Biaglow *et al.* reported that the adsorption capacity of Degussa P25 titania was 4.0×10^{-6} mol m^{-2} (25), which compares favorably to 4.5×10^{-6} mol m^{-2} determined in this work. However, Biaglow *et al.* found that only 40% of the 2-propanol converted to propene (25), whereas we observed that 70% converted to propene. Kim *et al.* also found that 4.2×10^{-6} mol m^{-2} of 2-propanol adsorbed on low-surface-area (10 $m^2 g^{-1}$) anatase with 48% being converted to propene during temperature-programmed reaction (26). The adsorption capacity of our titania prepared by hydrolysis of titanium isopropoxide is significantly higher than that of Degussa P25. Kim *et al.* suggest that steric effects influence the adsorption capacity of 2-propanol on titania surfaces since methanol, ethanol, and *n*-propanol adsorb to a greater extent (26). Evidently, the surfaces of our synthetic titania must be highly irregular to allow for a 30% greater adsorption capacity compared to P25. This conclusions is consistent with results from X-ray diffraction indicating that the sample is poorly crystallized anatase. Two additional conclusions can be derived from the results in Fig. 2 and Table 1. First, the adsorption capacities of the mixed oxides for 2-propanol are lower than that of pure titania and decrease with increasing Si content. An analogous trend is also seen in the ammonia adsorption capacities of the samples. Second, the percentage of 2-propanol reacted is significantly affected by the composition of the mixed oxides; silica-rich mixed oxides are much less reactive than titania-rich mixed oxides. The 40% lower adsorption capacity for 2-propanol of Ti : Si 6 : 1 compared to pure titania demonstrates the rather large affect of incorporating small amounts of silica into titania. A recent XPS study of titania–silica mixed oxides revealed that Si is preferentially located at the surfaces of Ti-rich mixed oxides, which may account for their relatively high surface areas (27). Indeed, the tripling of surface area (Table 1) and the dramatic decrease in Lewis acidity (Fig. 6) upon silica incorporation into titania both support the idea that silica is located at the surface of titania-rich mixed oxides. Although the total alcohol adsorption capacity decreases with incorporation of Si, the percentage of 2-propanol that reacts appears to be much more sensitive to the mixed oxide composition. As shown in Fig. 2, the adsorbate–surface interactions with Ti : Si 1 : 8 are not strong enough to dehydrate 2-propanol significantly. Therefore, the weak acid strength of a silica-rich mixed oxide determined by ammonia TPD and IR spectroscopy is corroberated by its low reactivity for 2-propanol dehydration.

Titania–silica mixed oxides are known to catalyze the isomerization of 1-butene at higher specific rates than either silica or titania (3, 4, 5). Titania-rich mixed oxides, in particular, were found to have the highest activities for the reaction (3, 4). Since the *cis/trans* ratio of the product butenes is near unity in all cases, the reaction is assumed to be acid-catalyzed, proceeding through a 2-butyl carbonium ion intermediate. This conclusion is supported by the work of Ko *et al.*, who found that treating a Ti–Si mixed oxide catalyst with water increased the specific activity of the sample for olefin isomerization (4). Nakabayashi also concluded from IR spectroscopy of adsorbed pyridine that new Brønsted acid sites accounted for the increase in the butene isomeration rate over a Ti–Si mixed oxide compared to the pure metal oxides (5). In our work, we used IR spectroscopy of adsorbed ammonia to evaluate the different types of acid sites on Ti–Si mixed oxides. Similar to Nakabayashi (5), we did not observe any Brønsted acidity on the surfaces of pure silica and pure titania. However, significant Brønsted acidity was detected on all the mixed oxides, titania-rich and silica-rich. Since the Ti-rich mixed oxides were the most active for butene isomerization, we conclude that 1-butene isomerization is enhanced by the formation of new Brønsted acid sites not present on pure titania. However, the weak Brønsted acid sites on the silica-rich mixed oxides are apparently not effective for butene isomerization.

Explanations for the generation of surface acidity on mixed oxides have been proposed (28, 29), but perhaps the most frequently referred to hypothesis is that of Tanabe *et al.* (30). A major assumption of their hypothesis is that the coordination number of each metal cation in its pure oxide structure is retained when the metal oxides are chemically mixed. In addition, the coordination number of every oxygen in the mixed oxide is assumed to be the coordination number of oxygen in the pure component oxide that is present in the majority. According to the above assumptions, a charge difference must exist on the impurity cation when octahedrally coordinated titania is mixed with tetrahedrally coordinated silica. Tanabe *et al.* suggested that if the charge difference is positive, then the impurity cation will act as a Lewis acid site, whereas if the charge difference is negative, then surface protons will balance the excess negative charge, producing Brønsted acidity (30). Thus, this hypothesis suggests that Lewis acidity will appear on titania-rich mixed oxides, while Brønsted acidity will appear on silica-rich mixed oxides.

Two problems that arise when this hypothesis is applied to Ti–Si mixed oxides can be resolved with the results

reported here. First, a positive charge on Si is calculated to appear for Ti-rich mixed oxides, but the hypothesis of Tanabe *et al.* does not require electroneutrality for this case (30). We observed by FT-IR absorption spectroscopy of adsorbed ammonia that Brønsted acid sites that are not normally present on pure titania appear on Ti-rich mixed oxides. In addition, Lewis acidity is greatly suppressed on the mixed oxide, as shown conclusively in Fig. 6. We propose that the positive charge difference that occurs when tetrahedral Si (in silica) mixes chemically with octahedral Ti (in titania) is balanced by hydroxyl groups, thus producing Brønsted acidity. This structure–property relationship is supported by results from the catalytic isomerization of 1-butene which indicate that Ti-rich mixed oxides are more active than pure oxides because of these new Brønsted sites.

The second problem that must be resolved is the dramatic decrease in surface reactivity of the Si-rich mixed oxide samples. According to Tanabe *et al.* (30), these materials should also exhibit pronounced surface acidity. Our structural investigation of Si-rich mixed oxides by EXAFS, XANES, UV, FT-IR and Raman spectroscopies indicated that Ti atoms no longer reside in octahedral sites, but instead substitute directly for Si atoms in tetrahedral sites (12). Therefore, the charge difference calculated by Tanabe *et al.* for Si-rich mixed oxides is based on the incorrect assumption that Ti maintains its octahedral coordination environment. A charge balance on a Si-rich mixed oxide using the experimental finding that Ti isomorphously substitutes for Si reveals no charge difference at all. Therefore, little surface acidity is expected on the Si-rich materials, which is consistent with the low reactivities of these materials for both 2-propanol dehydration and 1-butene isomerization. The adsorbate bonding interaction on silica-rich samples should also be fairly weak, which is consistent with low ammonia TPD peak temperatures for these materials.

Our previous microstructural investigation of Ti : Si 1 : 8 indicated that at least 70% of the Ti atoms reside in sites of tetrahedral coordination whereas the remaining atoms reside in nontetrahedral sites (12). If we can estimate the number of Brønsted and Lewis acid sites on Ti : Si 1 : 8, a quantitative structure–property relationship can be proposed. Fortunately, the IR spectrum in Fig. 6 for pure titania indicates that only Lewis acid sites are present on the surface. Combining the quantitative results from ammonia TPD with the integrated peak area for pure titania, we calculate the molar extinction coefficient for the Lewis acid peak to be 2.6 cm μmol^{-1}. Using this value and the results from IR spectroscopy and TPD of adsorbed ammonia for the mixed oxides, we can estimate the extinction coefficient of the Brønsted acid peak and the fraction of each acid type on the surface. This calculation assumes that the extinction coefficients of the Lewis and Brønsted acid peaks are independent of the oxide surface composition and the surface coverage, which might not be entirely valid. However, since the wavenumber positions of both peaks do not shift significantly with oxide composition, the extinction coefficients are likely to be fairly constant from sample to sample. Indeed, the average extinction coefficient of the Brønsted acid peak was calculated to be 2 cm μmol^{-1}, which compares to 3 cm μmol^{-1} calculated from ammonia adsorption on Brønsted sites in acidic zeolites (31). Our results also indicate that more than 80% of the ammonia molecules on the Ti–Si mixed oxides at 373 K are adsorbed on Brønsted acid sites. In addition, the ratio $NH_{3(ads)}$/Ti on Ti : Si 1 : 8 is nearly 30% which is about the same as the ratio of nontetrahedral Ti atoms in the sample. Thus, we conclude that at least one Brønsted acid site is associated with each nontetrahedral Ti atom in the sample.

The hypothesis of Tanabe *et al.* predicts that two protons are needed for each octahedrally coordinated Ti atom in a silica-rich mixed oxide in order to maintain electroneutrality. By observing the effect of dehydration on the XANES and UV reflectance spectra of Ti–Si mixed oxides, we concluded that a large fraction of the Ti atoms in Ti : Si 1 : 8 are located at the surface (12). However, we cannot rule out the possibility that some Ti atoms are located in the bulk structure. Therefore, perhaps some of the protons associated with nontetrahedral Ti atoms reside at sites that are inaccessible to ammonia. In addition, maybe only one of the two protons predicted by Tanabe *et al.* (30) is able to protonate ammonia at 373 K. As discussed earlier, the IR spectra in Fig. 5 indicate that the Brønsted sites on silica-rich mixed oxides are weaker in acid strength than sites on titania-rich samples. The spectra in Fig. 4 also support this idea since the surface hydroxyl groups of silica-rich mixed oxides are similar to those of pure silica, which do not function as Brønsted acid sites. However, the nontetrahedral Ti atoms in the silica-rich mixed oxide might be coordinated to only five oxygen atoms instead of the six assumed by Tanabe *et al.* (30). Only one proton is needed to balance the charge around a 5-coordinate Ti atom in a silica matrix. Unfortunately, our structural characterization is not able to determine unambiguously whether the nontetrahedral Ti atoms in Ti : Si 1 : 8 are coordinated to five or six oxygen atoms (12). Nevertheless, based on the quantitative results presented here, we suggest that nontetrahehrally coordinated Ti atoms in a silica matrix account for Brønsted acidity on Ti–Si mixed oxides.

Our results are also completely consistent with the lack of strong acidity in titanosilicalite molecular sieves. In these materials, Ti atoms substitute isomorphously for Si in the silicalite molecular sieve framework, thus creating unique sites for selective oxidation reactions with hydrogen peroxide. The lack of significant acidity on the titano-

silicalites nearly eliminates unwanted acid-catalyzed side reactions during oxidation reactions (32). Since all the titanium atoms in the molecular sieves are tetrahedrally coordinated, Brønsted acid sites are not expected on these materials. Indeed, infrared spectroscopy of pyridine adsorbed on titanium silicalite reveals only weak Lewis acid sites (33). We also examined the IR spectrum of ammonia adsorbed on TS-1 titanosilicalite. After our standard pretreatment and exposure to ammonia, we immediately observed a single peak associated with ammonia adsorbed on Lewis acid sites. Since most of the ammonia desorbed from the sample after purging the IR cell for several hours with N_2 at 373 K, we conclude that the tetrahedrally coordinated Ti atoms in TS-1 are fairly weak Lewis acid sites.

As mentioned earlier, there is little agreement on the strengths and number densities of acid sites on mixed oxides. We expect that surface acidity will be greatly affected by the synthesis procedure. Preparation methods involving coprecipitation of various reagents like titanium tetrachloride and sodium silicate may leave residual ions on the catalyst surface after washing that might affect surface acidity (19). In addition, rapid precipitation and high-temperature calcination may result in the formation of separate titania and silica phases. Therefore, our samples were prepared by controlled hydrolysis of metal alkoxides followed by calcination at 673 K. Strongly acidic Lewis sites may not have been exposed on our mixed oxide surfaces due to the relatively mild calcination temperature (673 K) compared to other studies. We anticipate that treatment of our samples at very high temperatures will dehydroxylate the surfaces more completely, thus exposing Lewis acid sites different than those present on the oxides after low-temperature calcination. However, the stability of our chemically mixed Ti : Si mixed oxides against phase segregation at high temperatures has not been evaluated. Also, Ti cations can be reduced from the 4+ state to the 3+ state by thermal treatments. Since the acidity of mixed oxides depends strongly on atomic-level mixing and the degree of surface hydroxylation, the wide variety of results presented in the literature is not surprising.

CONCLUSION

Results from this work indicate that the number density and relative strength of surface acid sites on titania are exclusively of the Lewis type, whereas the acid sites on the mixed oxides are mostly of the Brønsted type. These Brønsted sites increase the 1-butene isomerization activity over titania-rich mixed oxides compared to titania. However, the 1-butene isomerization activity decreases as greater amounts of silica are incorporated into the samples. This drop in activity over silica-rich catalysts results from a large fraction of the Ti atoms substituting directly for Si atoms in the tetrahedral network of silica. We suggest that the local charge imbalance associated with non-tetrahedral Ti atoms in the silica-rich samples accounts for the presence of Brønsted acid sites found by ammonia TPD and IR spectroscopy. In contrast to the results of some researchers, no strong Lewis acid sites were observed on any of the mixed oxides. Apparently, different synthesis conditions and subsequent thermal treatments are responsible for the variety of results concerning the acidity of Ti–Si mixed oxides.

ACKNOWLEDGMENTS

This work was funded by a National Science Foundation Young Investigator Award (CTS-9257306). Acknowledgement is also made to the donors of the Petroleum Research Fund, administered by the American Chemical Society (Grant ACS-PRF 24446-G5) and to the E.I. duPont de Nemours Co. for partial support of this research. We thank Degussa Inc. for donating P25 titania.

REFERENCES

1. Sheldon, R. A., and Van Doorn, J. A., *J. Catal.* **31,** 427 (1973).
2. Sheldon, R. A., *J. Mol. Catal.* **7,** 107 (1980).
3. Itoh, M., Hattori, H., and Tanabe, K., *J. Catal.* **35,** 225 (1974).
4. Ko, E. I., Chen, J. P., and Weissman, J. G., *J. Catal.* **105,** 511 (1987).
5. Nakabayashi, H., *Bull. Chem. Soc. Jpn.* **65,** 914 (1992).
6. Sohn, J. R., and Jang, H. J., *J. Catal.* **132,** 563 (1991).
7. Imamura, S., Tarumoto, H., and Ishida, S., *Ind. Eng. Chem. Res.* **28,** 1449 (1989).
8. Greegor, R. B., Lytle, F. W., Sandstrom, D. R., Wong, J., and Schultz, P., *J. Non-Cryst. Sol.* **55,** 27 (1983).
9. Schraml-Marth, M., Walther, K. L., Wokaun, A., Handy, B. E., and Baiker, A., J. *Non-Cryst. Sol.* **143,** 93 (1992).
10. Walther, K. L., Wokaun, A., Handy, B. E., and Baiker, A., *J. Non-cryst. Sol.* **134,** 47 (1991).
11. Ko, E. I., *Chem Tech* **Apr.** 31 (1993).
12. Liu, Z., and Davis, R. J., *J. Phys. Chem.* **98,** 1253 (1994).
13. Odenbrand, C. U. I., Andersson, S. L. T., Andersson, L. A. H., Brandin, J. G. M., and Busca, G., *J. Catal.* **125,** 541 (1990).
14. Primet, M., Pichat, P., and Mathieu, M.-V., *J. Phys. Chem.* **75,** 1216 (1971).
15. Busca, G., Saussey, H., Saur, O., Lavalley, J. C., and Lorenzelli, V., *Appl. Catal.* **14,** 245 (1985).
16. Nakamoto, K. "Infrared and Raman Spectra of Inorganic and Coordination Compounds," 4th ed., p. 191. Wiley, New York, 1986.
17. Primet, M., Pichat, P., and Mathieu, M.-V., *J. Phys. Chem.* **75,** 1221 (1971).
18. Dines, T. J., Rochester, C. H., and Ward, A. M., *J. Chem. Soc., Faraday Trans.* **87,** 643 (1991).
19. Odenbrand, C. U. I., Brandin, J. G. M., and Busca, G., *J. Catal.* **135,** 505 (1992).
20. Shibata, K., Kiyoura, T., Kitagawa, J., Sumiyoshi, T., and Tanabe, K., *Bull. Chem Soc. Jpn.* **46,** 2985 (1973).
21. Nakabayashi, H., Kakuta, N., and Ueno, A., *Bull. Chem. Soc. Jpn.* **64,** 2428 (1991).
22. Sabu, K. R. P., Rao, K. V. C., and Nair, C. G. R., *Bull. Chem. Soc. Jpn.* **64,** 1920 (1991).
23. Juskelis, M. V., Slanga, J. P., Roberie, T. G., and Peters, A. W., *J. Catal.* **138,** 391 (1992).

24. Nishiwaki, K., Kakuta, N., Ueno, A., and Nakabayashi, H., *J. Catal.* **118,** 498 (1989).
25. Biaglow, A. I., Gorte, R. J., Srinivasan, S., and Datye, A. K., *Catal. Lett.* **13,** 313 (1992).
26. Kim, K. S., Barteau, M. A., and Farneth, W. E., *Langmuir* **4,** 533 (1988).
27. Stakheev, A. Yu, Shpiro, E. S., and Apijok, J., *J. Phys. Chem.* **97,** 5668 (1993).
28. Kung, H. H., *J. Solid State Chem.* **52,** 191 (1984).
29. Kataoka, T., and Dumesic, J. A., *J. Catal.* **112,** 66 (1988).
30. Tanabe, K., Sumiyoshi, T., Shibata, K., Kiyoura, T., and Kitagawa, J., *Bull. Chem. Soc. Jpn.* **47,** 1064 (1974).
31. Martin, A., Wolf, U., Berndt, H., and Lucke, B., *Zeolites* **13,** 309 (1993).
32. Clerici, M. G., Bellussi, G., and Romano, U., *J. Catal.* **129,** 159 (1991).
33. Bittar, A., Adnot, A., Sayari, A., and Kaliaguine, S., *Res. Chem. Intermed.* **18,** 49 (1992).